Journal of Nuclear Materials 382 (2008) 126–133

Contents lists available at ScienceDirect

Journal of Nuclear Materials

journal homepage: www.elsevier.com/locate/jnucmat

Formation of stable sessile interstitial complexes in reactions between glissile dislocation loops in bcc Fe

Dmitry Terentyev [a,*], Lorenzo Malerba [a], Peter Klaver [b], Par Olsson [c]

[a] SCK-CEN, Nuclear Materials Science Institute, Boeretang 200, 2400 Mol, Belgium
[b] Queen's University Belfast, School of Mathematics and Physics, Belfast BT7 1NN, Northern Ireland, United Kingdom
[c] EDF, Department Matériaux et Méchanique des Composants, Les Renardieres, F-77250 Moret-sur-Loing, France

ARTICLE INFO

PACS:
61.82.Bg
75.50.Bb
61.72.Ji

ABSTRACT

Clusters of self-interstitial atoms (loops) are commonly observed in the microstructure of irradiated metals. These clusters can be formed directly in high-energy displacement cascades or by growth as a result of interaction between individual self interstitials. The majority of these clusters have features of glissile dislocation loops and migrate by fast one-dimensional glide. In this paper, we present results of a systematic molecular dynamics (MD) study of reactions involving glissile interstitial loops. By the example of bcc iron we demonstrate that the reactions can produce a number of specific, stable microstructural features, with different properties compared to the reactants. Namely, the reactions between the most common glissile clusters of ⟨1 1 1⟩ crowdions can result in coarsening or formation of immobile self interstitial complexes. The coarsening leads to a decrease of the total dislocation line length and therefore is favourable. The structure and stability of the junction formed in the reactions has been studied using many-body potentials and density functional theory (DFT) techniques. No evidence of the formation of a ⟨1 0 0⟩ loop from two glissile ⟨1 1 1⟩ clusters was found among the studied reactions. The immobile self interstitial complexes that form as a result of these reaction have, however, high binding energies, of the order of tens of eV, implying that a relatively long life time should be assigned to the resulting configurations and therefore that such objects are expected to contribute to the evolution of the microstructure under irradiation.

1. Introduction

Transition bcc metals and their alloys are the basis for structural materials used in present-day commercial power plants, as well as for current candidates to be exploited in future nuclear power plants [1]. During operation these materials will be subjected to high flux irradiation by fast neutrons, with subsequent formation of vacancies, self-interstitial atoms (SIAs) and their clusters. These clusters can be created either by reactions between individual SIAs or directly in high-energy displacement cascades [2,3]. While vacancy clusters are known to exhibit low mobility, SIA clusters of even considerable sizes can still migrate by fast one-dimensional glide [2,3]. Being highly mobile, these clusters take part in numerous reactions between themselves and with other microstructural features, such as dislocations, grain boundaries, precipitates and impurities. These radiation induced changes in the microstructure result in a significant degradation of the mechanical and physical properties of the materials. This has been the subject of intense studies, aimed at developing predictive models for the description of radiation effects [3]. To date, these models do not include, however, any reliable information about the specific interactions between SIA clusters. It is therefore important to obtain some systematic knowledge about SIA cluster interactions, as essential input for such models. This information cannot be directly obtained either from experiment, or from e.g. elasticity theory, due to the very small space and time scales (a few nanometres and picoseconds to nanoseconds) that are involved.

One of the most promising techniques to study nanoscale processes is believed to be atomistic modelling using computer simulation, in conjunction with modern developments of solid-state physics in the description of interatomic interactions [4]. SIA cluster properties have therefore been studied intensively by mainly molecular dynamics (MD) over the last decade and valuable information has already been obtained, including the results on some specific clusters–cluster reactions in pure Fe [5,6]. In particular, it has been shown that the coalescence of two glissile ½⟨1 1 1⟩ SIA clusters leads to the formation of an immobile complex whose stability is expected to be rather high and whose junction is of ⟨1 0 0⟩ character [5]. Based on this observation, a mechanism of nucleation of ⟨1 0 0⟩ loops in ferritic materials has been proposed, by suggesting that the merged glissile ½⟨1 1 1⟩ loops will gradually transform into a single entity

* Corresponding author. Tel.: +32 14 333197; fax: +32 14 321216.
E-mail address: dterenty@sckcen.be (D. Terentyev).

0022-3115/$ - see front matter © 2008 Elsevier B.V. All rights reserved.
doi:10.1016/j.jnucmat.2008.08.031

with $b = \langle 100 \rangle$ within a given time, beyond the MD timeframe [6]. The reactions between SIA clusters in the mentioned work were, however, studied only qualitatively and the available quantitative information on cluster–cluster interactions is currently not detailed enough to be extended to general cases when a number of parameters are involved. In this paper we present the results of a fairly systematic MD study of the mutual interaction between SIA clusters in a bcc Fe lattice. Comparative calculations have been carried out using two recent interatomic potentials (Ackland et al. [7] and Dudarev and Derlet [8]) known to be significantly improved in comparison with previously existing ones, especially regarding the description of self-interstitial defects. Additionally, density functional theory (DFT) calculations were performed to estimate the stability of the elementary defect which was found in the structure of the junction formed by the merging of the two reacting SIA clusters. The main goal of this work is the characterization of mechanisms and energies involved in the mutual interaction between SIA clusters as functions of their sizes and interaction geometry. Structures, stability and mobility of the products of different reactions between SIA clusters are the subject of the present study as well. It must be noted that the interatomic potential (IAP) derived by Dudarev and Derlet was especially fitted to allow explicitly for the effect of magnetism in bcc Fe. The obtained results are expected to be used further in the parameterization of microstructure evolution models such as object kinetic Monte-Carlo techniques.

2. Computational method

MD simulations of SIA clusters in bcc Fe crystals were employed using the most advanced IAPs developed for bcc iron to date [7,8], which qualitatively and quantitatively describe much better the properties of the single SIA and of small SIA clusters compared to *ab initio* predictions [9]. Both are standard many-body embedded atom method type potentials, but the IAP derived by Ackland et al. (henceforth potential A) has a cut-off interaction radius of 5.3 Å, while the cut-off of the IAP of Dudarev and Derlet [8] (henceforth potential D) is shorter by about 1.5 Å. A comparative study of the structure and interactions between dislocation loops and point-defects using the same IAPs has been recently reported elsewhere [10]. The used MD crystals contained up to 10^6 mobile atoms and standard 3D periodic boundary conditions (PBC) were applied. The reaction between pairs of SIA clusters consisting of $\langle 111 \rangle$ crowdions were simulated both at zero and finite temperature. These clusters can be described as small dislocation loops with Burgers vector $\boldsymbol{b} = \frac{1}{2}\langle 111 \rangle$ [2]. Two clusters with intersecting glide prisms were first created and then either the MD crystal was relaxed to the minimum potential energy applying a quench procedure for static calculations or the crystal was equilibrated at the temperature of interest for dynamic simulations. In the case of simulations at finite temperature, after equilibration the system was allowed to evolve as an NVE micro-canonical ensemble (N is the number of particles, V is the volume and E is the total energy of the system, parameters that remain constant in this ensemble during the simulation). The lattice constant was varied depending on the temperature, by making sure that the average pressure in the system equals zero. The temperature was varied from 0 to 600 K, when the intention was to study the final reaction product, and to higher temperatures (up to 1200 K) to study possible thermally activated transformations of the obtained reaction products. The interaction energy as a function of distance between clusters and reaction products was also extracted from this study. As in previous work [5], we have considered two possible geometries of intersecting cluster's glide prisms characterized by *acute* (71°) or *obtuse* (109°) angles between the cluster Burgers vectors, as shown in Fig. 1(a) and (b), respectively. Geometries corresponding

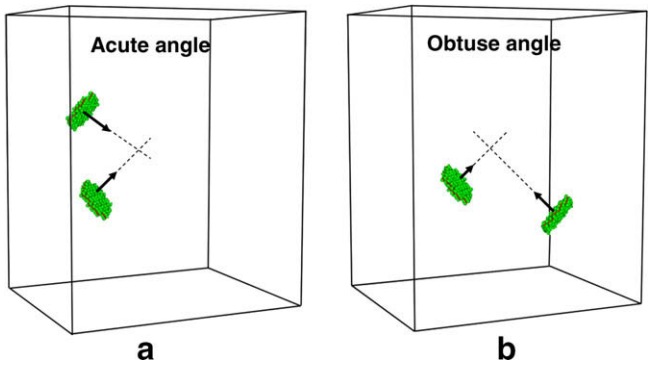

Fig. 1. Geometry of cluster–cluster interaction for (a) *acute* and (b) *obtuse* angles between their Burgers vectors.

to parallel Burgers vectors were not considered because, when the two glide prisms overlap in this case, the interaction is known to be purely repulsive [5]. We have studied clusters of regular hexagonal shape containing from 7 to 91-SIAs over a temperature range from 0 to 900 K within a simulation time of about 10 ns. Since $\frac{1}{2}\langle 111 \rangle$ loops have a long elastic strain field, extended along their Burgers vector direction, the simulation crystal was chosen to be a parallelepiped, in order to prevent the interaction of SIA clusters with their images via PBC. The orientation of the SIA clusters (i.e. the orientation of the crowdions forming the cluster) was defined via visualization of the defects present in the crystal. The determination of the space positions of the SIAs and of the orientation of each particular SIA (which can be $\langle 100 \rangle$, $\langle 110 \rangle$ or $\langle 111 \rangle$) was performed using the Wigner–Seitz cell method. The binding energy, E_b, between two interacting clusters was estimated by calculating the total energy of the system after a complete relaxation of the atoms at 0 K, using the following expression:

$$E_b = (E^{N_0}_{coh} + E^{N_1}_f + E^{N_2}_f) - E^N_{cur}, \quad (1)$$

where E^N_{cur} is the energy of a crystal consisting of N atoms and containing the two interacting clusters, $E^{N_1}_f$ is the formation energy of cluster #1 containing N_1 interstitials, $E^{N_2}_f$ is the formation energy of cluster #2 containing N_2 interstitials, $E^{N_0}_{coh}$ is the cohesive energy of the perfect crystal (i.e. free of defects) containing N_0 atoms. (Clearly, the condition of conservation of the number of atoms, $N = N_0 + N_1 + N_2$, must be fulfilled.) The formation energies of SIA clusters were estimated separately, using a standard procedure (e.g. [5]). In the case of finite temperature simulations, information on the position of the defects in the crystal as a function of simulation time has been extracted. In order to follow the cluster–cluster interaction process, visualization tools were employed and a subroutine of defect identification was called after each 10 fs to provide as precise a picture as possible. After the reaction was finished, the MD crystal was quenched to zero temperature so that the atomic structure of the reaction product could be studied in detail. To characterize the stability of the final products, additional MD simulations imitating thermal annealing were performed at different temperatures in smaller boxes, typically containing about half a million atoms, while the typical time involved in these simulations was about 10–20 ns.

3. Results

As was found earlier [5,6], the result of a cluster–cluster reaction depends on the intersecting geometry, the sizes of reacting clusters and the temperature. In general, the interaction between two clusters leads either to the formation of a stable, immobile complex consisting of SIAs oriented in different directions, or to the coalescence of the two SIA clusters, with the formation of a

big glissile cluster consisting of ⟨1 1 1⟩ crowdions. The latter occurs if one of the reacting clusters is significantly smaller than the other, as in this case the smaller cluster is absorbed by the bigger one. If the SIA clusters have comparable sizes, on the other hand, the formation of a stable, immobile SIA cluster occurs, whose life time depends on the sizes of the reacting clusters as well as on the temperature. The particular configuration (i.e. shape and structure) and the binding energy of this immobile complex depend on the angle (φ) between the two Burgers vectors of the reacting clusters, but in general the formed sessile configurations were observed to be stable for a substantial period of time (as much as is allowed by MD, i.e. tens of nano seconds) at relatively high temperatures (up to ~1000 K). Both applied IAPs were found to provide qualitatively similar results for reactions occurring under acute angle (AA). Discrepancies, however, exist for results obtained for the interaction under obtuse angle (OA). In addition, the applied IAPs predict different binding energies for the found immobile complexes. In what follows we give a detailed description and examples of each reaction observed, together with an evaluation of the stability of the products and a characterization of their structures. A quantitative comparison between results obtained using the two different IAPs and a discussion on the reliability of the obtained results and their possible implications concerning the microstructure evolution will be given in Section 4.

3.1. Interaction under acute angle, AA ($\varphi \sim 70°$)

Two different reactions were observed for this geometry: one in which the coalescence of the two clusters leads to the absorption of the smaller cluster by the bigger one and another one leading to the formation of a sessile cluster. In the former case, the smaller cluster changes the orientation of its crowdions to that of the bigger cluster, which is equivalent to flipping its Burgers vector. The result of the reaction is therefore a grown cluster with Burgers vector equal to that of the larger reacting cluster. Such reactions were observed for the following pairs of SIA clusters: 7–61, 7–91 and 19–91. If both reacting clusters are small and comparable in size, the resulting product is a three-dimensional, sphere-like, immobile SIA cluster consisting of ⟨1 1 0⟩ dumbbells having different orientations. An example of this reaction between two 7-SIA clusters is shown in Fig. 2. Reactions of this type were observed for the following pairs of SIA clusters: 5–5, 7–7 and 10–10 SIAs. The reaction between two 7-SIA clusters has been studied in detail at different temperatures and the formed sessile cluster was found to turn into a perfect glissile cluster at temperatures above 500 K within 10 ns. The final direction of the crowdions can be any of the possible ⟨1 1 1⟩ directions and is not related to the direction of either initial cluster. It is interesting to note that some of the interstitials present in the complex shown in Fig. 2 form the non parallel configuration (NPC) of di-SIA shown in Fig. 3(a) and reported earlier [11]. In this configuration, three atoms share one atomic site and lie in a {1 1 1} plane, at variance with the 'canonical' configurations shown in Fig. 3(b) and (c), where the dumbbells or crowdions are parallel. These NPC of SIA clusters in Fe are studied in detail in [12].

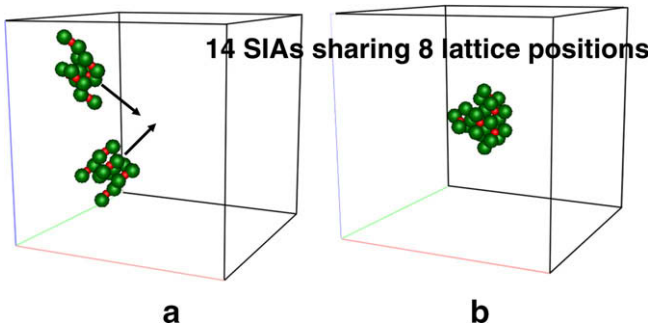

Fig. 2. Reaction between two 7-SIA clusters under acute angle between cluster's Burgers vectors. The product is a thermally unstable sphere-like cluster.

When the glide prisms of larger SIA clusters intersect, during simultaneous motion of the clusters towards each other, their habit planes (HP) rotate from {1 1 1} to {1 1 0}, while the initial orientations of the crowdions in the clusters are preserved. When they finally approach and join with one another, they lie in the same {1 1 0} HP and create a junction line in a ⟨1 1 0⟩ direction. Snapshots extracted from MD simulations of the interaction of two 91-SIA clusters are presented in Fig. 4. The formed junction consists of the above-mentioned NPC of di-SIAs; this time, however, the three atoms sharing one lattice site lie in a {1 1 0} plane instead of a {1 1 1} plane. The cross-section of the formed complex after the reaction between two 91-SIA clusters (see Fig. 4) is shown in Fig. 5(a). It can be seen that two parts of the complex (cluster A and cluster B) contain crowdions with different orientations, while the junction consists of di-SIAs in NPC. This type of reaction was observed for reacting clusters containing more than 19 SIAs and the product of such a reaction will be referred to later on as a *sessile-parallel* configuration, because it cannot glide and the HPs of two merged clusters are parallel to each other. This sessile-parallel complex is fairly stable, since no structural transformations were observed during annealing at 900 K over 10 ns. At higher temperatures (above 1000 K), however, it does transform into a perfect glissile ⟨1 1 1⟩ cluster within a few nanoseconds. The transformation occurs via partial propagation of the junction in one of the two parts of the sessile complex and by subsequent reorientation of the crowdions in this part. Then the junction consisting of NPC di-SIAs is transformed into a platelet of single ⟨1 1 1⟩ crowdions by emitting self interstitials, which merge very quickly at the edge of the SIA cluster within the next 10 ns.

It should be noted that static calculations revealed that all the reactions occurring under the AA proceed spontaneously without any energy barrier. The dynamic calculations confirmed this, as

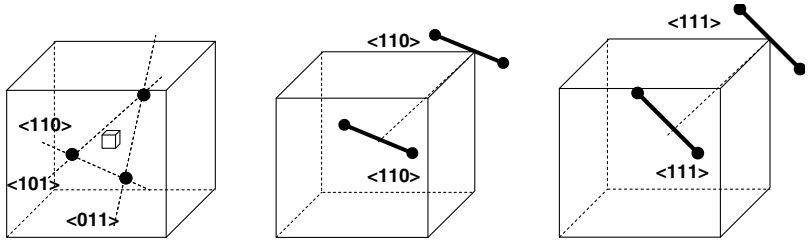

(a) Non parallel di-SIA reported in [11]

(b) Parallel di-SIA made of ⟨110⟩ dumbbells

(c) Parallel di-SIA made of ⟨111⟩ crowdions

Fig. 3. Different configuration of di-SIA clusters.

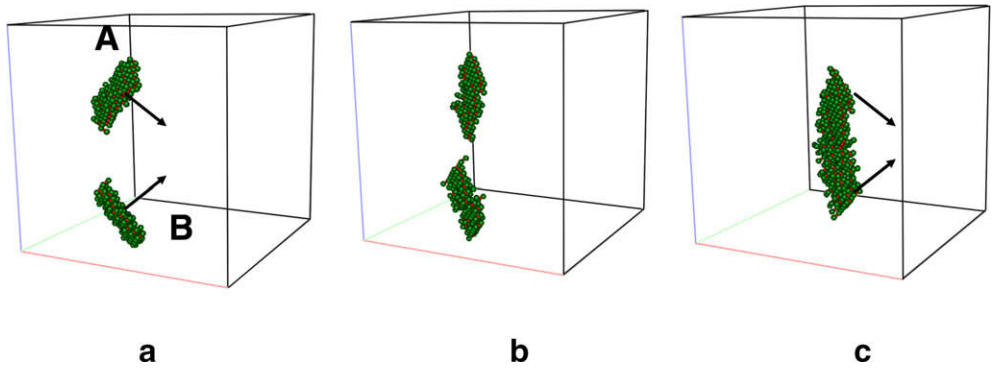

Fig. 4. The reaction between two 91-SIA clusters under *acute* angle.

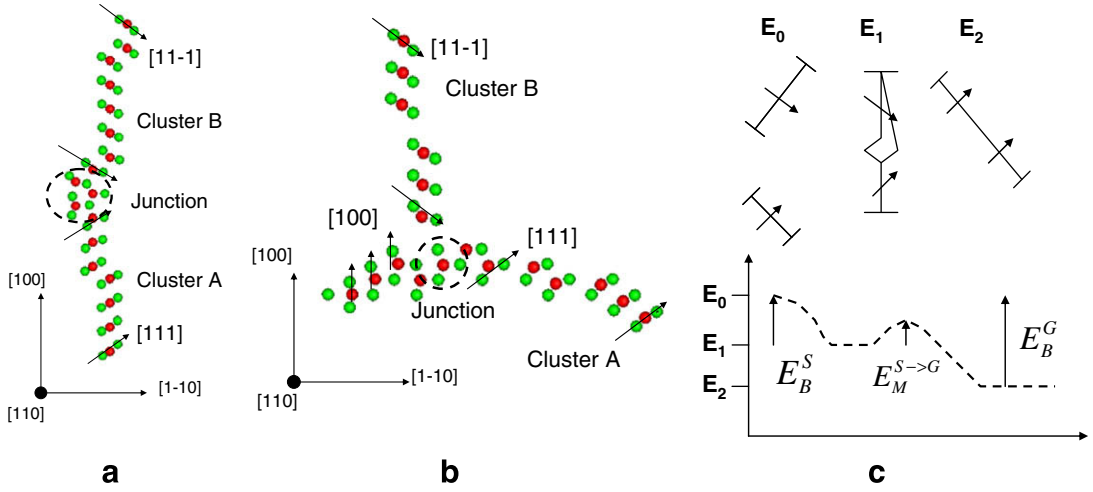

Fig. 5. The cross-section in the (1 1 0) plane of the formed sessile clusters after the reactions between two 91-SIA clusters under acute (a) and obtuse (b) angles. Interstitial atoms are light-green circles and lattice sites are dark-red circles. Black arrows show the direction of the crowdions in the parts of the clusters A and B, the dashed circle displays the junction, which is aligned along the [1 1 0] direction. The energy landscape for the studied reactions, including subsequent transformation into glissile cluster, is schematically shown in (c). (For interpretation of the references to colour in this figure legend, the reader is referred to the web version of this article.)

the two reacting SIA clusters were always observed to move towards each other simultaneously, without time delay and independently of their sizes or of temperature, in all studied cases.

3.2. Interaction under obtuse angle, OA ($\varphi \sim 109°$)

As in the case of AA reactions, the interaction between small SIA clusters leads to the formation of 3D-sessile complexes, like the one shown in Fig. 2(b). If there is a significant difference between the sizes of the interacting clusters, the absorption of the smaller cluster occurs, but in this case the motion of the clusters towards the intersection point is not simultaneous, like in the case of the reaction under AA. First, the smaller cluster moves to the edge of the glide prism of the bigger cluster and only then does the bigger cluster move towards the smaller one. Thereafter, coalescence with the formation of one big glissile cluster occurs.

For large SIA clusters of comparable sizes a different reaction was observed. At the beginning of the reaction, one of the clusters (A) moves towards the edge of the glide prism of the other one (B) and after that cluster approaches A. Prior to coalescence, the HP of

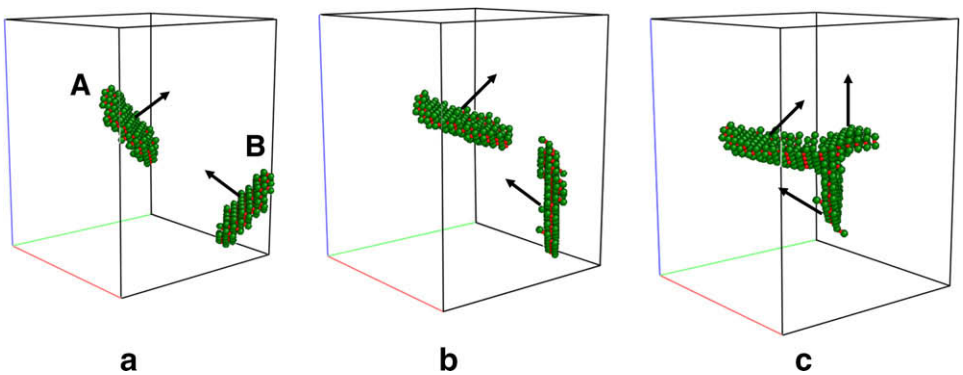

Fig. 6. The reaction between two 91-SIA clusters under *obtuse* angle.

the moving cluster B rotates from the initial {111} to a {110} plane. After this, the cluster A moves through the glide prism of the cluster B and the HP of cluster A rotates from the initial {111} to a {100} plane, as shown in Fig. 6(a). Then coalescence leading to the formation of the configuration of two crossing SIA clusters occurs, as shown in Fig. 6(b) and (c). The product of this reaction contains three different parts and each part is a nearly planar object, as can be seen from Fig. 6(c). The cross-section of the complex given in Fig. 6(c) is presented in Fig. 5(b), where all three different parts are clearly seen. One part, (cluster A), lies in this case in the (001) plane and contains crowdions oriented along the [111] direction; the second one, (cluster B), lies in the $(1\bar{1}0)$ plane and contains crowdions oriented along the $[11\bar{1}]$ direction; the third part consists of the junction line and a *tail* from cluster A and is formed by di-SIA in the NPC. Note that this third part can be also represented as a double layer of dumbbells oriented along the [100] direction, as shown in Fig. 5(b). Hereafter, the product of this reaction will be referred to as a *sessile-perpendicular* configuration, since the HPs of the reacting clusters are perpendicular to each other. The annealing of this sessile-perpendicular configuration has revealed that the complex turns first into a sessile-parallel configuration (see Fig. 4(b)) by the bowing of the segment lying on the {100} plane and subsequently rotating the HP into the {110} plane. Such a transformation occurs above 1000 K within 10 ns. Thereafter, the sessile complex transforms into the glissile SIA cluster in the manner already described in Section 3.2.

3.3. Stability of the reaction products

From the results presented above it follows that the sessile SIA complexes produced in the cluster–cluster reactions, though highly stable, finally transform into glissile ⟨111⟩ SIA clusters. This implies that the reaction products are metastable configurations, while the most stable state remains a platelet of ⟨111⟩ crowdions. No thermally activated transformation into a plain cluster containing ⟨100⟩ interstitials has been observed, in contrast to what has been suggested in [6] as possible outcome for similar reactions.

A measure of the stability of the sessile reaction products is their binding energy, E_B^S, defined as $E_B^S = E_0 - E_1$, which can be estimated using static calculations at 0 K. Here, E_0 is the energy of the system containing the two non-interacting reactants, while E_1 is the energy of the system when the reaction is finished i.e. when the sessile complex is formed. The results are presented in Table 1, from which it is clearly seen that all of the observed reactions between SIA clusters lower the energy of the system. It is interesting to note that the binding energies of the sessile complexes mainly depend on the sizes of interacting clusters, but not on the intersecting geometry. In fact it was found that the binding energy corresponding to the sessile state does not grow linearly with increasing sizes of the reacting clusters and that it depends directly on the length of the junction line, as shown in Fig. 7, suggesting that the formation of the junction is the main reason for the binding of the two clusters and that the stability of the junction largely determines the stability of the complex. Indeed, the formation of the junction leads to a decrease of the total length of dislocation lines in the system (dislocation density), since four out of twelve dislocation segments (each SIA cluster has six edge dislocation $(a/2\langle 111\rangle)$ segments) are transformed into a junction line. The longer the junction, the larger the decrease of dislocation density. This observation can be used to explain why the formation of the sessile complexes was not observed in the reactions between SIA clusters with considerable differences in size, for at least two possible reasons. Firstly, in the reaction between small and large SIA clusters the length of the junction is too short to provide substantial binding and this is why the smaller cluster would be absorbed almost immediately by the larger one. Secondly, the energy required to flip the crowdions in small clusters (of size about 7-SIAs) is sufficiently low, so that the corresponding rotation may occur in the vicinity of another large SIA cluster.

Table 1
Binding energies of sessile complexes formed in acute and obtuse angle reactions, estimated using static calculations with the two interatomic potentials

Reaction	Potential D		Potential A	
	Product	E_B (eV)	Product	E_B (eV)
Results for acute angle reactions				
7 + 7	3D-sessile	3.85	3D-sessile	4.46
19 + 19	Sessile-parallel	5.74	Sessile-parallel	6.12
19 + 37	Sessile-parallel	6.28	Sessile-parallel	8.80
37 + 37	Sessile-parallel	10.38	Sessile-parallel	9.81
7 + 91	Glissile	7.4	Glissile	8.26
61 + 61	Sessile-parallel	10.65	Sessile-parallel	14.6
37 + 91	Sessile-parallel	9.69	Sessile-parallel	12.08
61 + 91	Sessile-parallel	12.18	Sessile-parallel	15.68
91 + 91	Sessile-parallel	13.89	Sessile-parallel	17.57
Results for obtuse angle reactions				
7 + 7	3D-sessile	3.85	3D-sessile	4.46
19 + 19	Sessile-parallel	5.74	Sessile-perpendicular	6.68
19 + 37	Sessile-perpendicular	6.2	Sessile-perpendicular	8.68
37 + 37	Sessile-perpendicular	8.83	Sessile-perpendicular	10.36
61 + 61	Sessile-perpendicular	9.25	Sessile-perpendicular	13.84
37 + 91	Sessile-parallel	9.69	Sessile-perpendicular	11.01
61 + 91	Sessile-parallel	12.18	Sessile-perpendicular	14.87
91 + 91	Sessile-perpendicular	11.91	Sessile-perpendicular	16.46

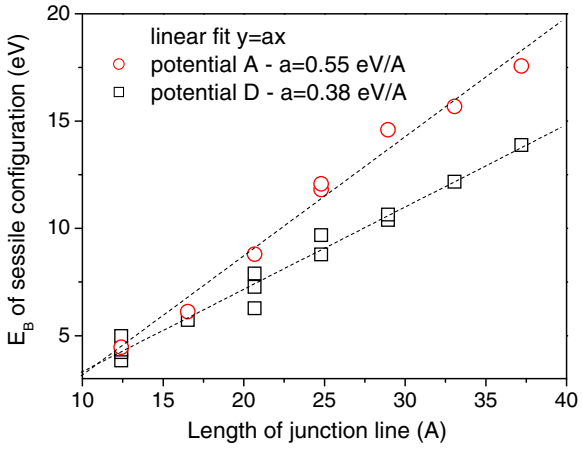

Fig. 7. The binding energies of the sessile complexes as functions of the junction length, estimated by static calculations using both potentials A and D.

The formation energies of two separate clusters (E_0), of the sessile complexes formed in the AA reaction (E_1) and of the SIA clusters after transformation to a glissile configuration (E_2) are displayed in Fig. 8 versus the total number of self interstitials present in the system. It is clear that the formed sessile clusters are metastable states, while the most stable configuration is always a glissile ⟨111⟩ cluster. The energetics of the reactions between pairs of SIA clusters is schematically represented in Fig. 5(c). While initially the pair of non-interacting SIA clusters has formation energy E_0, the spontaneous (i.e. without energy barrier) formation of sessile complexes lowers the total energy of the system by a value of $E_0 - E_1$ (binding energy), which we have seen depends on the length of the junction. For the transformation of the metastable sessile complex into a glissile cluster, with formation energy E_2, an energy barrier, $E_M^{G\to S}$, needs to be overcome, as shown in Fig. 5(c). The stability, and therefore the life time, of the sessile complexes will depend on the difference between the binding

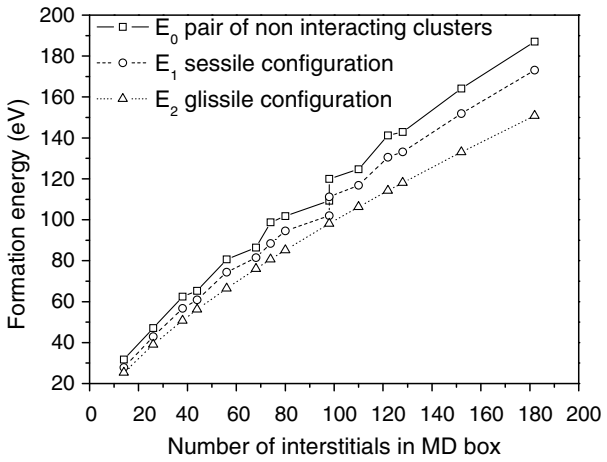

Fig. 8. The formation energies of: pairs of non-interacting clusters, sessile-parallel complexes and glissile clusters versus number of SIA present in the system, estimated by static calculations using potential D. Qualitatively similar results are found using potential A.

energies corresponding to the glissile state, $E_B^G = E_0 - E_2$, and the metastable sessile state E_B^S. The smaller the difference $(E_B^G - E_B^S)$, the more stable is the sessile configuration. So far, however, nothing can be said about the quantity of the energy barrier, $E_M^{G\to S}$ for the transformation from the sessile into the glissile configuration, which decides the kinetics of the process.

In order to estimate this barrier, additional simulations of high temperature annealing were performed at different temperatures using potential A in the specific case of the parallel sessile complexes formed in the reaction between two 37-SIAs clusters. The time it takes for the sessile configurations to be transformed into the glissile ones versus temperature is given in Fig. 9. The corresponding activation energies and logarithms of the prefactors were deduced by regression to be 1.5 ± 0.21 eV/1.65 ± 0.17 eV and $-16.37/-17.48$ for acute and obtuse angle reactions, respectively. From these numbers a rough estimate of the time required for the same transformation of the same sessile clusters to occur at 600 K, supposing that the effect of entropy at high temperature is small, can be extrapolated to be between 1.2 and 5.7 ms. Interstitial-type complexes that remain immobile for times of this order of magnitude are thus expected to have a significant influence on the microstructure evolution, because instead of migrating rapidly

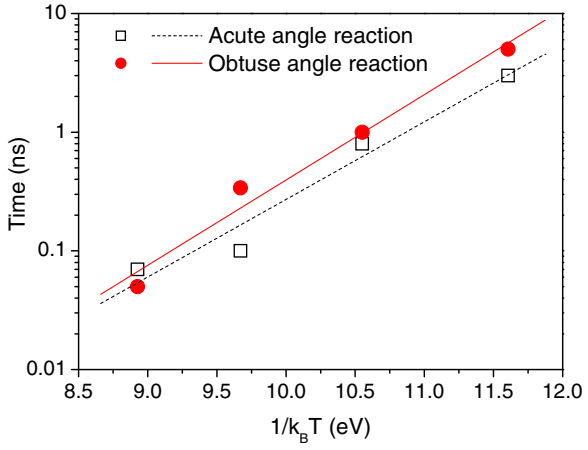

Fig. 9. Time required for sessile clusters formed in the reaction between two 37-SIAs clusters under different geometries to transform into a glissile ½⟨1 1 1⟩ cluster (MD simulations performed using potential A).

to sinks, as glissile clusters would do, they can act during their life time as effective sinks for point-defects and mobile point-defect clusters.

3.4. Comparison between the two potentials and with DFT calculations

Table 1 shows that some qualitative and quantitative discrepancies between the results obtained with the two used IAPs exist. First of all, not all of the considered OA reactions with potential D lead to the formation of the sessile-perpendicular configuration. While the results obtained with potential A are highly systematic, i.e. the AA reaction leads invariably to the formation of the sessile-parallel complex and the sessile-perpendicular complex is always formed in the OA reaction (if the reacting clusters contain more than 19 SIA), this is not the case for potential D. Secondly, while the results obtained with both IAPs suggest that the sessile-parallel configuration is more stable than the sessile-perpendicular one, the binding energies of the sessile-parallel configurations with a junction line of the same length are slightly higher with potential A than with potential D (see Fig. 9). It therefore seems that the two IAPs predict different junction line formation energies.

Attempts at studying the junction line as an isolated defect failed because, without the presence of the remainder of the interacting clusters, the junction is unstable. However, it has already been noticed that the elementary unit of the junction line is the di-SIA in the NPC presented in Fig. 3(a), slightly rotated to lie in a {1 1 0} plane. The formation energy and binding energy of this configuration was therefore used to assess the different junction stability predicted by the two IAPs and to compare this result with DFT calculations. These were carried out using VASP [13], a plane-wave code that implements the projector augmented wave (PAW) method [14,15]. Standard PAW potentials supplied with VASP were used, with exchange and correlation described by the Perdew–Wang parameterisation in the generalised gradient approximation [16]. An Fe potential with 8 valence electrons was used. The plane-wave energy cut-off was set to 300 eV, which was found to be sufficient for convergence of energy. The Brillouin zone sampling was done in meshes of $3 \times 3 \times 3$ k-points, using the Monkhorst–Pack scheme. The single SIA and di-SIA clusters in different configurations were relaxed in $5 \times 5 \times 5$ bcc unit supercells (250 atoms). During ionic relaxation, the supercells were held at constant volume corresponding to the pure Fe equilibrium lattice parameter. The same conditions, i.e. constant volume calculations in a box of 250 atoms, were applied for the estimation of the formation energies of single and di-SIAs using the two IAPs. The results of this comparative study are given in Table 2. The formation energy of the di-SIA in the NPC is 0.06 eV lower for potential A and 0.1 eV lower for potential D than the formation energy of the ⟨1 1 1⟩ configuration. This is consistent with the fact that the former provides a somewhat more stable junction than the latter, although there are other factors determining the stability of the junction and therefore the binding energy between SIA clusters in a sessile configuration, expected in the final cluster product. It is however certainly noteworthy that according to DFT the NPC of the di-SIA corresponds to the ground state of the di-SIA (see also [12]). The possible consequences of this fact in terms of stability of the junctions of the sessile reaction products are discussed in the next section.

Aside from the estimate given in Fig. 9, the time required for the sessile configurations to transform into glissile ones was not systematically studied in the present work. However, the observed qualitative differences between the two potentials are in line with the observed lower stability of the junction according to D as compared to A. The annealing of the reaction products between 37–37, 61–61 and 91–91 pairs of SIA clusters, performed using potential A, has shown that the sessile-perpendicular complexes transform

Table 2
Formation energy of single and di-SIAs in different configurations, estimated by relaxation to zero temperature

	di-SIA ⟨110⟩ Fig. 2(a)	di-SIA ⟨110⟩ Fig. 2(b)	di-SIA ⟨111⟩ Fig. 2(c)	Single SIA ⟨110⟩
Potential A	6.61 (0.49)	6.31 (0.79)	6.67 (0.43)	3.55
Potential D	6.80 (0.5)	6.37 (0.93)	6.90 (0.4)	3.65
DFT (VASP)	7.04 (0.82)	7.15 (0.81)	Not calculated	3.93

All calculations were performed at constant volume in a box containing 250 atoms. The binding energy of each configuration is given next to the formation energy in parenthesis. All values are given in eV.

into sessile-parallel and then immediately after to glissile configurations within 10 ns at temperatures above 1000 K. Conversely, if potential D was employed, the transformation from the perpendicular to the parallel configuration was observed at about 400–500 K, within the same timeframe (i.e. 10 ns), while the final transformation to the glissile state occurred at about 800–900 K. Thus, the two IAPs provide not only different stability for the sessile configurations, but also different energy barriers for the sessile-to-glissile transformation, potential A giving higher values. In addition, potential D seems to penalise the stability of the sessile-perpendicular configuration versus the sessile-parallel one, and this explains while not all OA reactions led to the formation of the former.

It should be also added that the range of interaction between SIA clusters is relatively long and predicted to be approximately the same by both applied IAPs. While the interaction range does not depend on the geometry of the interaction, it strongly depends on the sizes of the reacting clusters. For example, in the case of a reaction between two 91-SIA and two 7-SIAs clusters, a visible motion of the clusters towards the point of coalescence starts when the distance between them and the crossing point is less than 12 nm and 7 nm, respectively.

4. Discussion

As mentioned in the introduction, AA reactions have been qualitatively studied before and results were reported in [5,6], whereas the OA reactions have, to the authors best knowledge, never been studied before. It should be also noted that the formation of small 3D-sessile clusters consisting of perpendicular di-SIAs in the reactions between pairs of SIA clusters was never reported. The occurrence of the OA reactions and in general the differences with respect to earlier work found in the present one might be due to the properties of the new IAPs [7,8], which are significantly improved as compared to previous ones for bcc Fe [17,18].

Although the formation a ⟨100⟩ segment was indeed observed at the junction of the reaction product between two large enough clusters, in agreement with previous studies performed with earlier potentials [5,6], in the present work no formation of SIA clusters made of ⟨100⟩ dumbbells was detected as a result of a two-cluster reaction. Thus, the mechanism of formation of a ⟨100⟩ loop proposed earlier in [6] is here questioned, since the junction propagation and subsequent transformation of the sessile complex into a perfect ⟨100⟩ cluster was not observed to occur in the cases here analysed, not even at high temperature. Instead, as has been described in Section 3.3, all observed sessile complexes transformed into glissile clusters during thermal annealing. It is noteworthy that recent *in situ* TEM studies in pure Fe gave direct evidence of coalescence between small ½⟨111⟩ SIA dislocation loops, mediated by the temporary formation of a convoluted SIA cluster, before gradual transformation into a larger, perfect ½⟨111⟩ dislocation loop [19], in qualitative agreement with the present simulation results, while no formation of ⟨100⟩ loops as the final result of such a coalescence was found. Thus, while the mechanism of formation of ⟨100⟩ loops by ⟨100⟩ junction propagation proposed in [6] remains hypothetically possible, it is not corroborated by either simulation or experimental evidence, and the identification of the actual mechanism of ⟨100⟩ loop formation remains an outstanding issue. On the other hand, the long-range interaction between loops, when the motion of one cluster influences the motion of another one, with subsequent coalescence, as observed here, has been experimentally detected. These qualitative agreements should, however, be taken with caution, as the times involved in the TEM observations are substantially longer than the timeframe of MD simulations. TEM images of convoluted interstitial objects formed under irradiation in pure Fe have been reported also in another, earlier experimental study [20]. The interstitial clusters therein photographed remind of the sessile-perpendicular configuration shown in Fig. 6(b), even the plane orientations of the experimentally observed objects were just the same as in the sessile-perpendicular complexes found here. However, the size of the photographed objects is not comparable with the size of the objects simulated here.

Although the IAPs used here provide a much better description of SIA defects as compared to previous ones, some of the results presented here raise important questions related to their actual accuracy and reliability. Table 2 shows that the formation energies of the di-SIAs in different configurations, calculated using DFT and IAPs in exactly the same conditions, are not only quantitatively, but also, and more importantly, qualitatively different. According to the DFT results the NPC of the di-SIA is the most stable configuration; this fact is not reflected by the used IAPs and, most likely, it is not reflected by any of the currently existing (at least published) IAPs for pure Fe, since the presently used ones are known to be among the best fitted to the data on point-defects extracted from DFT. We have shown that the NPC of the di-SIA may play the role of stabilizer of the found sessile cluster reaction products, on the one hand, and is the building block for the formation of ⟨100⟩ segments, on the other. Consequently, a quantitatively reliable study of the stability of the observed sessile configurations and the evaluation of the energy barriers involved in the sessile-to-glissile transformations would require an as-correct-as-possible description of the NPC of the di-SIA, which neither IAP provides. For the moment it can therefore only be concluded that the stability of the observed small 3D-sessile clusters and large sessile configurations, as described by the IAP, is likely to be underestimated, compared to a hypothetical, currently unfeasible, DFT study. That is, the transformation time at 600 K roughly estimated to be on the order of ms at the end of Section 3.3, based on IAP results, may in reality be much longer. This, however, only underscores the importance of accounting for the existence of these immobile configurations in microstructure evolution models, since immobile objects having at least a life time of ms are expected to contribute significantly to the bulk microstructure development.

In addition, the obtained results suggest that a double layer of ⟨100⟩ dumbbell can be formed as a platelet of perpendicular di-SIAs. Since the DFT results suggest that this NPC of the di-SIA is the most stable one, further investigations on the mechanisms of growth of SIA clusters are probably needed. Maybe, after all, the junction propagation mechanism proposed in [6] could eventually turn out to be a more solid possibility than the present results seem to suggest.

Although it should be verified, it is likely that the general implications of the results presented here can be extended to other bcc alloys, where the formation of glissile dislocation loops occurs under irradiation and reactions involving their mutual interactions may lead to a decrease in the total dislocation line length, leading to the formation of sessile complexes. If so, the presence of interstitial loop complexes having totally different migration properties compared to fast glissile ones may be an important aspect

influencing the evolution and accumulation of radiation damage in bcc materials. Therefore, the possibility of the formation of sessile SIA complexes should not be disregarded in any model developed for the assessment and description of the irradiation-induced microstructure of bcc metals and alloys with a similar behaviour of glissile interstitial loops.

5. Conclusions

A few conclusions can be drawn relying on the results obtained in this work:

1. Glissile SIA clusters exhibit long-range, attractive interaction which leads to their coalescence (unless the Burgers vectors of the SIA clusters are parallel when the glide prisms overlap).
2. The result of the coalescence between pairs of glissile SIA clusters depends on the interaction geometry, sizes of the reacting clusters relative to each other and temperature, and it can lead to either the formation of a sessile complex or the direct transformation into a bigger glissile cluster. Small clusters coalesce by forming thermally unstable, sphere-like clusters.
3. The characteristic feature of all observed sessile complexes is the presence of a junction line consisting of di-SIAs in a non-parallel configuration. The same configuration is observed also in the thermally unstable, sphere-like clusters formed by the coalescence of small clusters. The binding energy attributed to the sessile SIA complex is proportional to the length of the junction line and therefore proportional to the number of di-SIAs formed, thus the stability of this di-SIA configuration is expected to dictate the stability of the junction and of the whole complex.
4. All of the observed sessile complexes were seen to transform into glissile $\langle 1\,1\,1\rangle$ clusters during annealing at high enough temperature. The time involved in the transformation seems to depends on the sizes of the reacting clusters relative to each other, as well as on the stability of the junction, at a given temperature. The transformation time was found to decrease exponentially by increasing the temperature, suggesting the occurrence of a thermally activated process with a characteristic activation energy.
5. The two IAPs used here in many cases provide qualitatively similar results. The potential D, which adopts a formalism that explicitly allows for magnetism, predicts however lower stability for the observed sessile complexes, as compared to the potential A. Neither potential provides high enough stability for the non-parallel di-SIA configuration, as compared to DFT calculations.
6. The possibility of formation of sessile SIA complexes should be included in microstructure evolution models for bcc metals and alloys with a similar behaviour of glissile interstitial loops.

Acknowledgements

This work, partially supported by the European Commission under the contract of Association between Euratom and the Belgian State, was carried out within the framework of the European Fusion Development Agreement (EFDA), task TTMS-007. This work was also partially supported by the European project PERFECT (FI60-CT-2003-508840).

References

[1] R. Klueh, D. Harries, High-Chromium Ferritic and Martensitic Steels Nuclear Applications, ASTM International, 2001. 337p.
[2] Yu.N. Osetsky, D.J. Bacon, A. Serra, B.N. Singh, S.I. Golubov, Philos. Mag. A 83 (2003) 61.
[3] B.N. Singh, S.I. Golubov, H. Trinkaus, A. Serra, Yu.N. Osetsky, A.V. Barashev, J. Nucl. Mater. 251 (1997) 107.
[4] N.M. Ghoniem, E.P. Busso, N. Kiosssis, H. Huang, Philos. Mag. 83 (2003) 3475.
[5] Yu.N. Osetsky, A. Serra, V. Priego, J. Nucl. Mater. 276 (2000) 202.
[6] J. Marian, B.D. Wirth, J.M. Perlado, Phys. Rev. Lett. 88 (2002) 255507.
[7] G.A. Ackland, M.I. Mendelev, D.J. Srolovitz, S. Han, A.V. Barashev, J. Phys.: Condens. Matter 16 (2004) 1.
[8] S. Dudarev, P. Derlet, J. Phys.: Condens. Matter 17 (2005) 7097.
[9] F. Willaime, C.C. Fu, M.C. Marinica, J. Dalla Torre, J. Nucl. Instrum. and Meth. B 228 (2005) 92.
[10] D. Terentyev, L. Malerba, J. Nucl. Mater. 377 (2008) 141.
[11] F. Gao, D.J. Bacon, Yu.N. Osetsky, P.E.J. Flewitt, T.A. Lewis, J. Nucl. Mater. 276 (2000) 213.
[12] D. Terentyev, T.P.C. Klaver, P. Olsson, M.-C. Marinica, F. Willaime, C. Domain, L. Malerba, Phys. Rev. Lett. 100 (2008) 145503.
[13] G. Kresse, J. Furthmuller, Phys. Rev. B 54 (1996) 11169.
[14] P.E. Blöchl, Phys. Rev. B 50 (1994) 17953.
[15] G. Kresse, D. Joubert, Phys. Rev. B 59 (1999) 1758.
[16] J.P. Perdew, Y. Wang, Phys. Rev. B 45 (1991) 13224.
[17] G.J. Ackland, D.J. Bacon, A.F. Calder, T. Harry, Philos. Mag. A 75 (1997) 713.
[18] M. Finnis, J. Sinclair, Philos. Mag. A 50 (1984) 45.
[19] K. Arakawa, M. Hatanaka, E. Kuramoto, K. Ono, H. Mori, Phys. Rev. Lett. 96 (2006) 125506.
[20] A.E. Ward, S.B. Fisher, J. Nucl. Mater. 166 (1989) 227.